RSC Advances

ROYAL SOCIETY OF CHEMISTRY

www.rsc.org/advances

EFFECTS OF DANGLING BONDS AND DIAMETER ON THE ELECTRONIC AND OPTICAL PROPERTIES OF InAs NANOWIRES

E. Gordanian,[a] S. Jalali-Asadabadi,[a,] IftikharAhmad,[b,c,**] S. Rahimi[a], and M. Yazdani-Kacoei[a]*

[a]*Department of Physics, Faculty of Science, University of Isfahan (UI), HezarGerib Avenue, Isfahan 81746-73441, Iran*

[b]*Center for Computational Materials Science, University of Malakand, Chakdara, Pakistan*

[c]*Department of Physics, University of Malakand, Chakdara, Pakistan*

** *Corresponding author:* *Iftikhar Ahmad Ph.D. (Idaho, USA)*
Professor of Theoretical Physics
Center for Computational Materials Science
University of Malakand,Chakdara, Pakistan
ahma5532@gmail.com
(092)332-906-7866

* saeid.jalali.asdabadi@gmail.com

ABSTRACT

In this article we explore the effects of dangling bonds and diameter on the electronic properties of the wurtzite InAs nanowires (NWs) using the density functional theory. The NWs are confined in the hexagonal supercell and are simulated in the [0001] direction. The calculations have been carried out by applying the periodic boundary conditions along the NW axis, i.e., z-Cartesian coordinate, providing enough vacuum to isolate the system from its neighbors. Optical properties of a material are directly related to the band-gap; therefore a relationship between the band-gap and diameter of the nanowires is obtained by using two models, where the band-gap for a larger diameter NW can be estimated. The results of these models are compared with each other and the effects of the dangling bonds on the band-gaps are also investigated. The band-gap of the nanowires decreases and the dangling bonds ratio increases with the increase in the diameter of the nanowire, and hence we expect that for large diameter nanowire the band-gap will approach to the band gap of the bulk material. An interesting feature of shift in the band-gap from indirect to direct, i.e. optically inactive to active, is also observed in these NWs with the increase in the diameter.

Key Words: InAs nanowires; electronic properties of InAs nanowires; dangling bonds; ab-initio calculations

I. INTRODUCTION

Semiconductor nanowires (NWs) have attracted considerable interest due to their fascinating optical and electrical properties originating from their one dimensional (1D) nanocrystal structure.[1–6] These semiconductor nanowires are used in technological applications, such as field-effect transistors, logical gates, biological sensors, lasers, light-emitting diodes, nanoscale inter-connects, and active components of photoelectronic devices and nano-electromechanical systems.[7,8]

The electrons in semiconductor nanowires are free to move along their axis and are confined within the NW diameters (D). Therefore, it is expected that quantization of energy occurs perpendicular to the NW axis. Thus, NW diameter may determine the electronic structure, and as a result the band gaps of the wires. In some cases, the band gaps of wires are related to their diameters by the relation, $1/D^2$.[9] In nanowires the edge and the surface atoms also influence the electronic structure of the material.[10]

The InAs nanowires can be experimentally grown using the vapor-liquid-solid mechanism with a gold particle seed. InAs nanowires are grown on different substrates with various methods like: metal organic chemical vapor deposition (MOCVD) and molecular beam epitaxy (MBE).[8,9] They have shown that the crystal structure of the nanowires is strongly dependent on the growth conditions and the experimental methods. InAs compound crystallizes in both, zinc blende (ZB) and wurtzite (WZ) phases. The former structure, i.e., ZB, is more stable phase in the bulk form of the compound, however, the stability is exchanged when the scale is reduced towards the nanometer, where theWZ becomes more stable than the ZB phase for the small diameters of InAs nanowires.[11]

In this paper, the band structures of the bulk and nanowires of InAs in the wurtzite phase are plotted in the [0001] direction to explore the electronic properties of the compound. The band-gaps are calculated for five samples of different diameters of the nanowires and by the extrapolation of the results, variation in the band-gap of the nanowires can be estimated for larger diameters by using two models. For the clear picture of the internal behavior of the NWs, their total density of states are plotted, while partial density of states are plotted for p and s orbitals of the center and surface indium and arsenic atoms. The calculations are carried out by utilizing the density functional theory (DFT)[12,13] using the WIEN2k[14] code. All the

calculations are performed at zero temperature and zero pressure. Furthermore, the edge atoms are not saturated by other atoms such as hydrogen.

II. COMPUTATIONAL DETAILS

In this work, all the calculations are carried out by using the density functional theory (DFT)[12,13] using the full-potential linearized augmented plane waves method[15] as embedded in the WIEN2k code[14]. For the exchange-correlation potential, the Perdew and Wang local density approximation[16](PW-LDA), the Perdew-Burke-Ernzerhof generalized gradient approximation[17] (PBE-GGA) and Engel-Vosko approximation[18] (EV) are used in the WIEN2k code. Full relaxation was exerted on all atoms until the total forces became smaller than 2 *mRy/Bohr*. The muffin-tin radii were chosen to be 2.2 a.u.for In and 2.1 a.u. for As atoms in NWs and 2.45 a.u. for both, In and As, in the bulk structure. The expansion of the wave functions and charge densities were cut off by the $R_{MT}K_{MAX}$= 7 and G_{MAX}= 12 parameters, respectively. We generated 4 special k-points in the first Brillouin zone (1BZ) corresponding to the shifted Monkhorst-Pack grids of 1×1×8 for integrations over the 1BZ of the NW super cell. Similarly, the mesh is also optimized and found to be 8 × 8 × 8 for the bulk system.

The calculated lattice parameters with LDA and GGA approximations for the wurtzite InAs, having space group p63mc21 are a = 4.26Å, c = 7.01 Å and a =4.36 Å, c = 7.13 Å, respectively.The LDA results for the lattice constants are in closer agreement with the experimental results, a= 4.284 Å and c = 6.996 Å[20], than the GGA. The calculated lattice parameters by the ultrasoft pseudopotential with LDA approximation are a = 4.327 Å, c = 7.092 Å[21] and a = 4.192 Å , c =6.844 Å[22]. As the LDA provides better lattice parameters, therefore this approximation is further used to simulate the InAs nanowires. The vacuum is optimized to 12 Å in order to prevent the interaction between the neighboring nanowires. After truncating the nanowire from the bulk, we have calculated forces on atoms and found them very large. To reduce the forces, we relaxed the supercell until the forces become less than 2 *mRy/Bohr*. It is important to notice that the accuracy of our non-passivated nanowire calculations can be increased by saturating nanowire surface bonds with a variety of the chemical functional groups such as -H, -OH and $–NH_2$. In anticipation of further investigations, we report our results for the non-passivated NWs.

All the modeled nanowires with different diameters before and after relaxation are shown in Fig.1. After relaxation, the As atoms on the surface moved out, so we observed outward relaxation, while the In atoms moved in, so the In atoms have inward relaxation. The movement of atoms depends on its electronegativity and hence furthest movement is observed in atoms with larger electronegativity (for example As than In atoms). The bond-length is also changed and the variation in bond-length on the surface and center of NWs is different. By increasing the diameter of NW the variation in the bond-length of the center is small, while in the large diameter NW it is usually equal to the bulk value. The C lattice parameter along the axis of the growth of the nanowires are optimized by calculating the supercell energies at different values of C and then fitting parabolic curve to the energy versus C parameter diagram, our calculated results are shown in Table 1. This behavior is a kind of surface effect that occurs in the supercell and this is the reason that why relaxation is an important effect due to the dangling bonds at the surface.

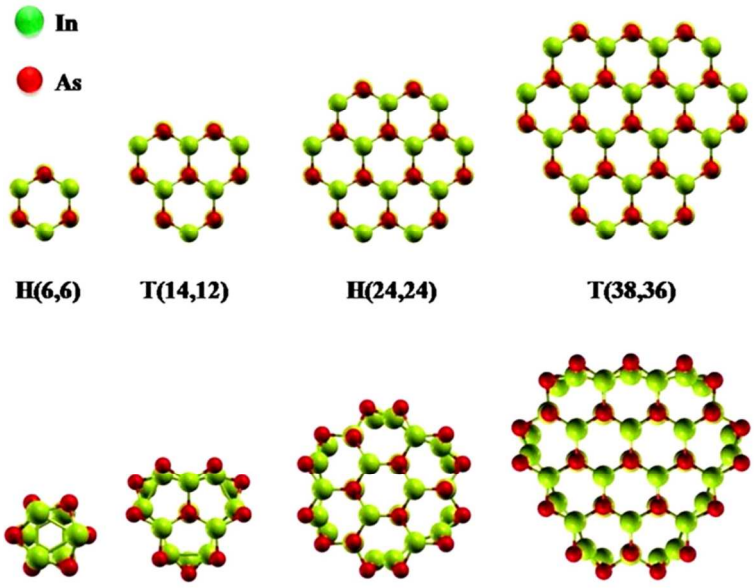

Fig. 1: (Colors online) Four first diameters of wurtzite NWs, up before and down after relaxations. The small (red) spheres are As atoms and the large (green) ones are In atoms. In each NWs H and T shows the hexagonal and trigonal, respectively and the numbers in parenthesis indicate the number of atoms in each layer.

TABLE 1: Optimized C lattice parameter for NWs.

System	Diameter (Å)	C-lattice parameter (Å)
Wz-H(6,6)	5.50	6.43
Wz-T(14,12)	8.95	6.77
Wz-H(24,24)	13.05	6.79
Wz-T(38,36)	17.20	6.89

III. RESULTS AND DISCUSSIONS

The crystals of InAs have two known phases, i.e., wurtzite and zinc blende. In the present paper we have focused our studies on the electronic properties of the wurtzite phase by various DFT based techniques; LDA, GGA and Engel-Vosko GGA (E-V). The calculated band gap for the bulk sample is compared with the experimental and other theoretical results in Table 2, while the band structure for the E-V approximation is plotted in Fig.2. The table reveals that the results of the E-V approximation is in better agreement with the experimental results, so we have used this approximation for the calculation of the electronic properties of the nanowires.

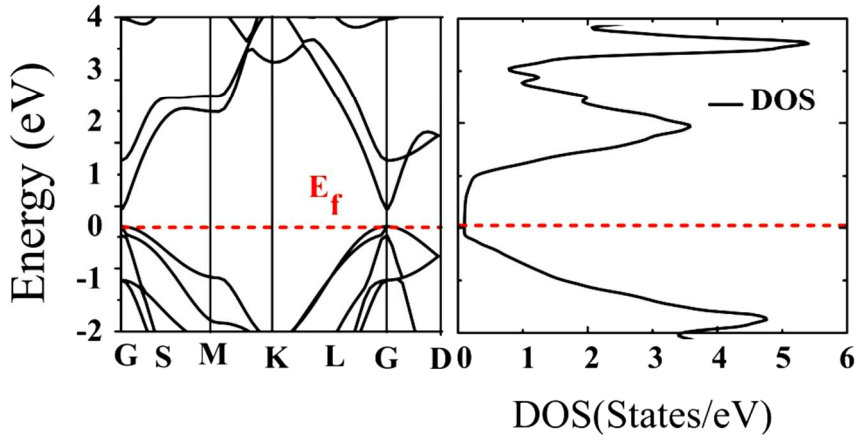

Fig. 2: (Colors online) The band structure and total density of states for InAs bulk. The Fermi energies are adjusted at zero.

TABLE 2: Band gap energy of bulk in wurtzite phase.

Method	E_{XC}	E_g(eV)
LAPW	LDA	0
LAPW	PBE-GGA	0
LAPW	EV-GGA	0.38
LAPW	TB-mBJ	0.68
[a]PPW	LDA	0
[b]GW		0.667
[c]Exp		0.520

[a]Reference 23; The data were calculated within the pseudopotential method as embodied in the VASP code.

[b]Reference19.

[c]Reference 23.

For the determination of the electronic properties of the NWs and investigation of the quantum confinement effect, the band-gaps of the nanowires are calculated by plotting their band structures in Fig.3. The results of the band-gaps are presented in Table 3. The band-gaps reveal that all theNWs are semiconductors with band-gaps larger than the band-gap of the bulk InAs.

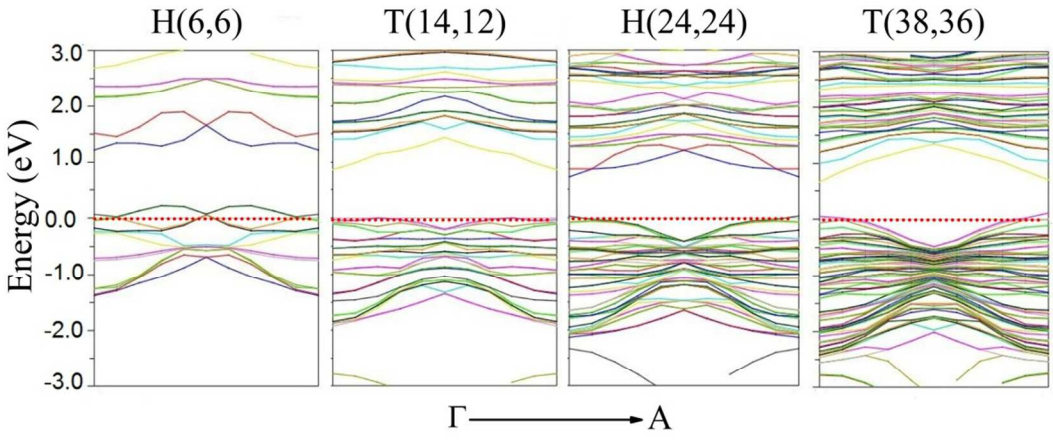

Fig. 3: (Colors online) Band structures of wurtzite NWs, the Fermi energies are adjusted at zero.

An interesting feature of shift in the band-gap from indirect to direct with the increase in the diameter is a unique property of these wutrzite InAs nanowires. It is clear from Table 3 that the band-gap of the nanowire changes with the change in its diameter. It is clear from Fig.3 that the nature of band-gap is indirect for nanowires with diameter smaller than 13 Å, i.e., for WZ-T(38,36), while for WZ-H(54,54) the band gap is direct at G symmetry point. The reason of the indirect band-gap for the small diameter InAS nanowires is the influence of surface atoms that miss their bonds on NWs which is more prominent in small diameter NWs as compared to the large diameters. Hence, by increasing the diameter, the effect of surface atoms becomes lesser than the small diameter ones, so for larger NWs the band-gap is direct.

The difference between the band-gaps of the NWs and bulk sample (ΔE_g) are clear from Table 4 as well as from Figs. 2 and 3. The results presented in the figures reveal that for all the nanowires under study except H(54,54), the valence band maximum (VBM) and level immediately below in energy (VBM-1) are degenerate levels with a high energy dispersion, while for H(54,54) both of them are nondegenerate and have high energy dispersions. Compared

TABLE 3. Band gap energy of nanowires in wurtzite phase.

System	Diameter (Å)	Gap type	Band gap energy (eV)
Wz-H(6,6)	5.50	indirect	0.998
Wz-T(14,12)	8.95	indirect	0.876
Wz-H(24,24)	13.05	indirect	0.795
Wz-T(38,36)	17.20	direct	0.742

TABLE 4. Variation in band gap of nanowires.

System	ΔE_g(eV)
H(6,6)	0.618
T(14,12)	0.496
H(24,24)	0.415
T(38,36)	0.362

with those for the bulk InAs, we note that VBM and VBM-1 are nondegenerate such as H(54,54). Except for T(38,36) and H(54,54), the levels at the top of the valence band for the InAs NWs have a great dispersion, that is indirect and different than the bulk InAs. So, we expect that the increase in the diameter of the nanowire will definitely change the behavior of the NWs band structure to the bulk sample.

The band structure for the wurtzite nanowires by passivation dangling bonds are plotted by Dos Santos et al.[24] and their results show that for all NWs the VBM and VBM-1 are nondegenerate and have low energy dispersion, so we could see the effect of passivation in band structure. The NWs have one type of dangling bond, shown in Fig.4. For the first, second, third, and fourth diameter of NWs; the variation in the band-gap increases. The increase in the variation in the band-gap in the small diameter nanowires may be due to the quantum confinement, which increases the energy separation among the sub-levels when the diameter decreases.

By decreasing the diameter of the NW, the In and As atoms gets closer to each other and the ratio of the dangling bonds in the supercell also becomes large. The variation in the band-gap versus dangling bonds ratio and diameter are plotted in Fig.5. The figure shows that the band-gap decreases and the dangling bonds ratio (number of dangling-bonds/total bands) increases with the increase in the diameter of the NW. So, we expect that for large diameter the NWs band-gap approach to the bulk material.

To estimate variation in the band-gap of the lager diameter nanowires, we use the EMA-PIB model, based on particle in a box to predict that how quantum confinement depends on the shape, so that we can evaluate the relation between variation in the band-gap and hole as well as electron effective mass. The EMA-PIB model uses particle in a box expression for the calculation of the kinetic confinement energy of quantum well, quantum dot and quantum wire, where the quantum wire variation band-gap is shown in Eq. (1):[25]

$$\Delta E_g = E_g^{NW} - E_g^{bulk} = 2.34\left(\frac{h^2}{8D^2}\right)\left(\frac{1}{m_e^*}+\frac{1}{m_h^*}\right) \quad \text{.....(1)}$$

where ΔE_g is the difference between NWs band-gap and bulk energy, h is the Planck's constant, D is NWs diameter and m_e^* and m_h^* are the effective masses of the electron and hole,

respectively. For the estimation of the constant term in Eq. (1), the band-gap versus D^{-2} is plotted in Fig. 6(a) by using the results of band-gaps in Table 4. By fitting linear function to this data and calculating its slope we could estimate the coefficient term in Eq. (1) and after that we can estimate the variation in band-gap for large diameters. We have plotted variation in the band-gap versus D in Fig.6(b) for larger diameters. However, deviations from this simple EMA-PIB model have been reported for small diameter semiconductor NWs[19], so we have used Eq.(2) for the estimation of the band-gap in the larger diameters NWs by using Eq.(2):

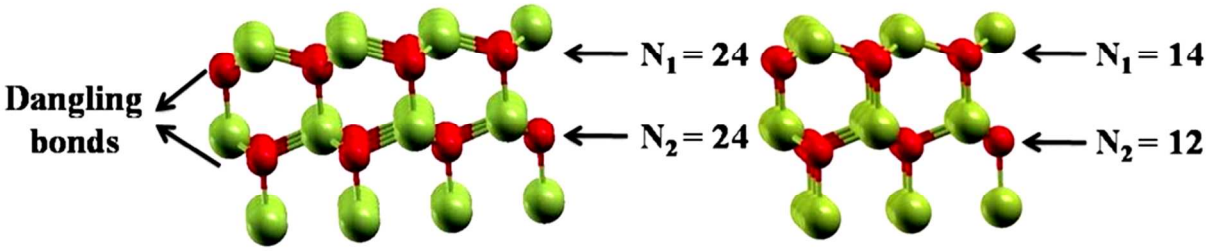

Fig. 4: (Colors online) Wurtzite dangling bonds.

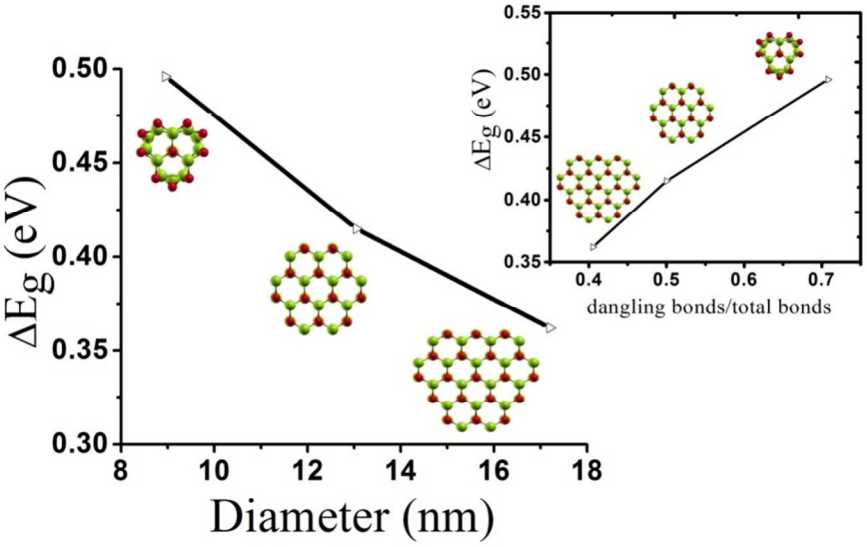

Fig. 5: (Colors online) Variation in band-gap versus NWs diameter and dangling bonds ratio.

$$E_g^{NW} = E_g^{bulk} + \frac{\beta}{D^{\alpha}} \quad \text{.....(2)}$$

α and β for the Wurtzite phase are evaluated by fitting a suitable function (allometric) to the calculated results of the band-gaps and diameters of NWs, which can be used to calculate the band-gap energy for larger diameter nanowires. Our Wurtzite results are plotted in Fig.7 and the evaluated values for α is 0.22066 and for β is 2.02088, where dos Santos et al.[8] obtained 0.81 and 1.94 values for α and β, respectively for the zinc blende phase of the InAs nanowires using pseudopotential method. By comparing the results of EMA-PIB model and Eq.(2) it is evident that for Eq.(2) a decrease in the variation in the band-gap is lower than that given by D^{-2}, with the values in Eq.(1).

The electronic arrangement of arsenic and indium are $[Ar]3d^{10}4s^24p^3$ and $[Kr]4d^{10}5s^25p^1$, respectively. For the determination of the electronic properties of InAs nanowires, first of all the partial density of states of the bulk material are plotted in Fig. 8. The total density of states of the InAs nanowires are plotted in Fig.9. For all the NWs the valence band is divided into two sub-

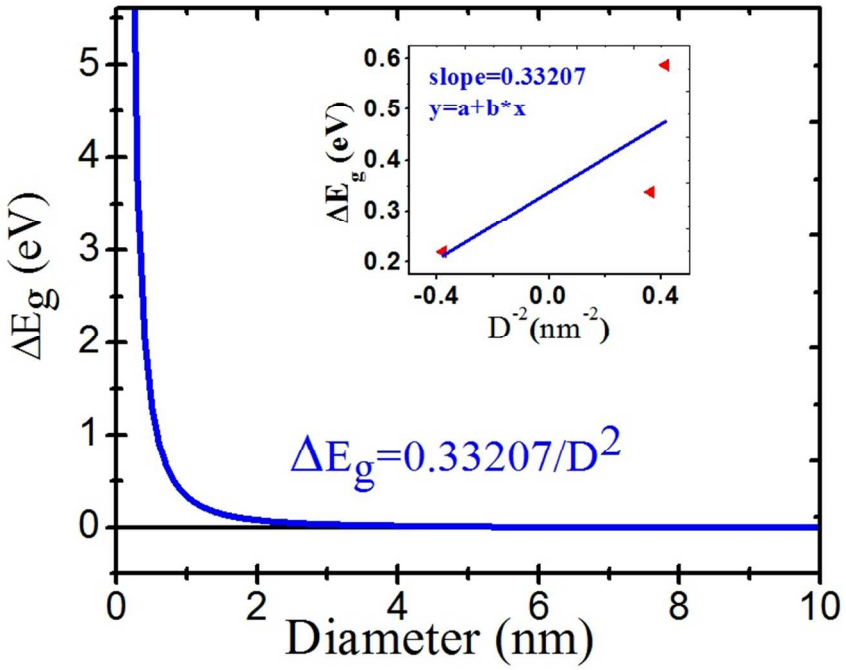

Fig. 6: (Colors online) Variation of band-gap of NWs versus D^{-2} and variation of band-gap with D of NWs by using EMA-PIB model.

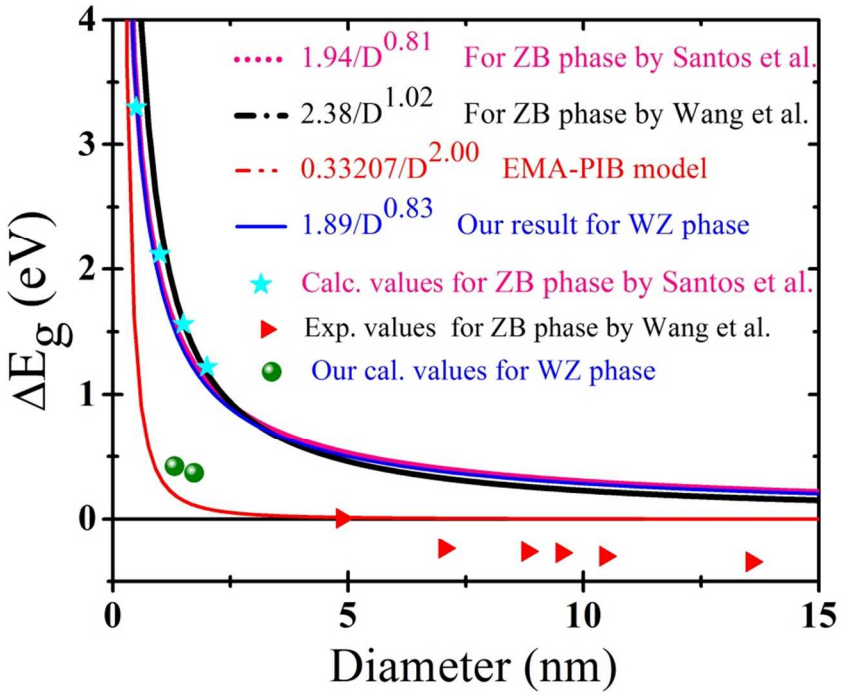

Fig. 7: (Colors online) Variation in the band-gap (ΔE_g) for the wurtzite NWs.

bands, so we have labeled starting from the top (zero energy) as VB1 and VB2. By increasing the NWs diameter the widths of these sub-bands is increased and the band-gap between VB1 and VB2 is decreased. To investigate the effect of the core and surface atoms in the total density of states, partial density of states for s and p orbitals of In and As surface and center atoms are plotted in Fig.10 except for the first diameter which has only surface atoms because of its small diameter. The partial density of states shows that for VB1 the 4p orbital of As overlaps with the 5p orbital of In, while the VB2 is formed by the overlap of the 4s orbital of As and 5s orbital of In. Because of the dangling-bonds in the surface, the average energy of the surface states is larger than the center states. It is clear from the total and partial DOS that, except for the H(6,6) which is the smallest nanostructure, the behavior of the highest occupied (HO) states does not change for all nanowires. In other words, the peak of surface states lies below the valence band

maximum and most likely this is the cause of the less reduced band gap with respect to the bulk value, where such results are also reported for BeS nanowires.[26]

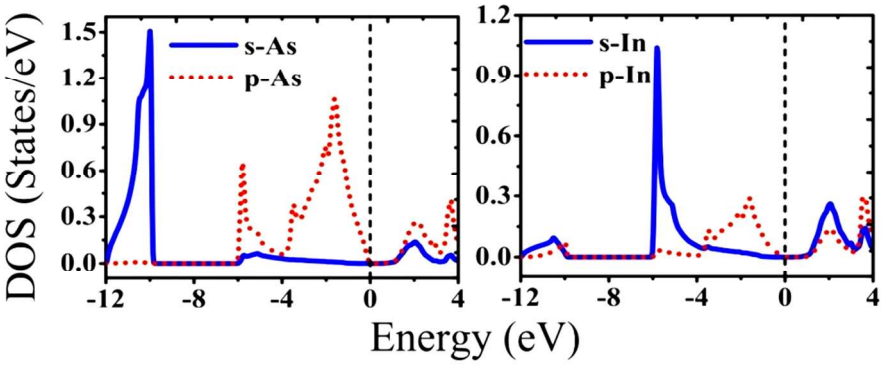

Fig. 8: (Colors online) Bulk InAs partial density of states.

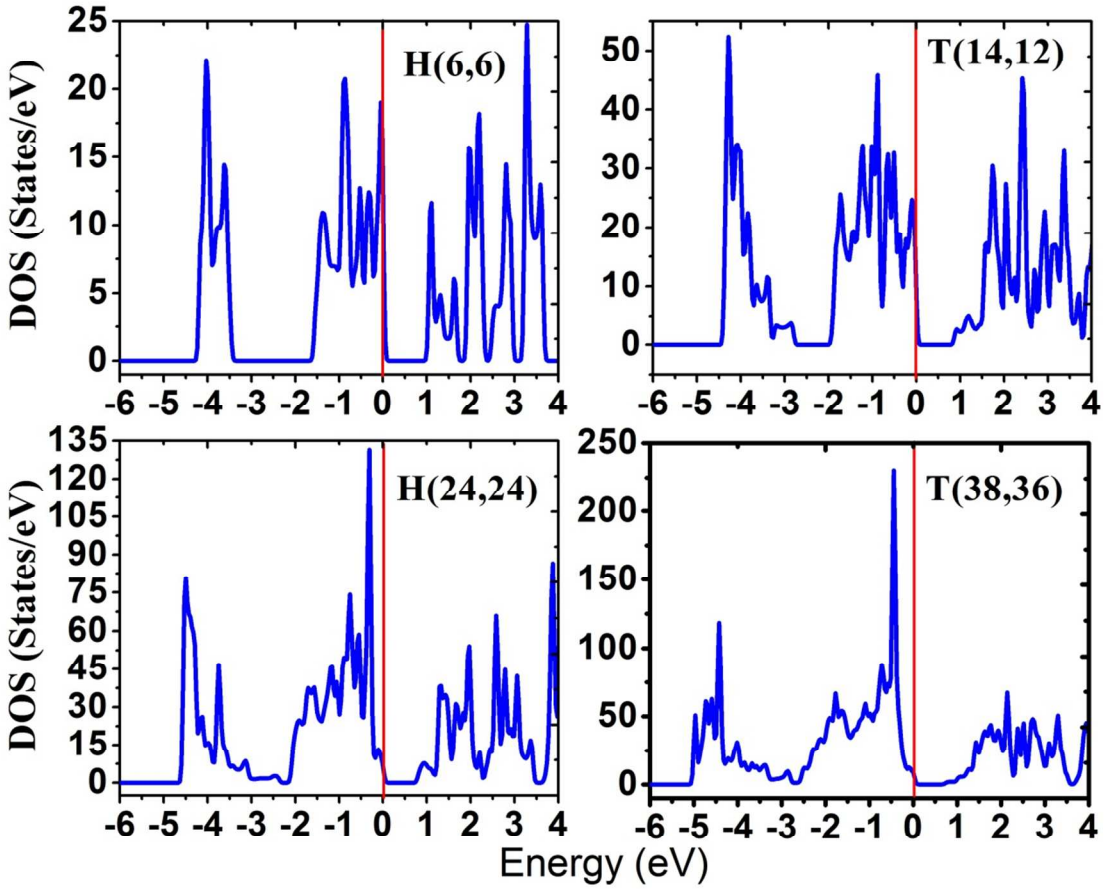

Fig. 9: (Colors online) Total density of states for the four first diameter of NWs.

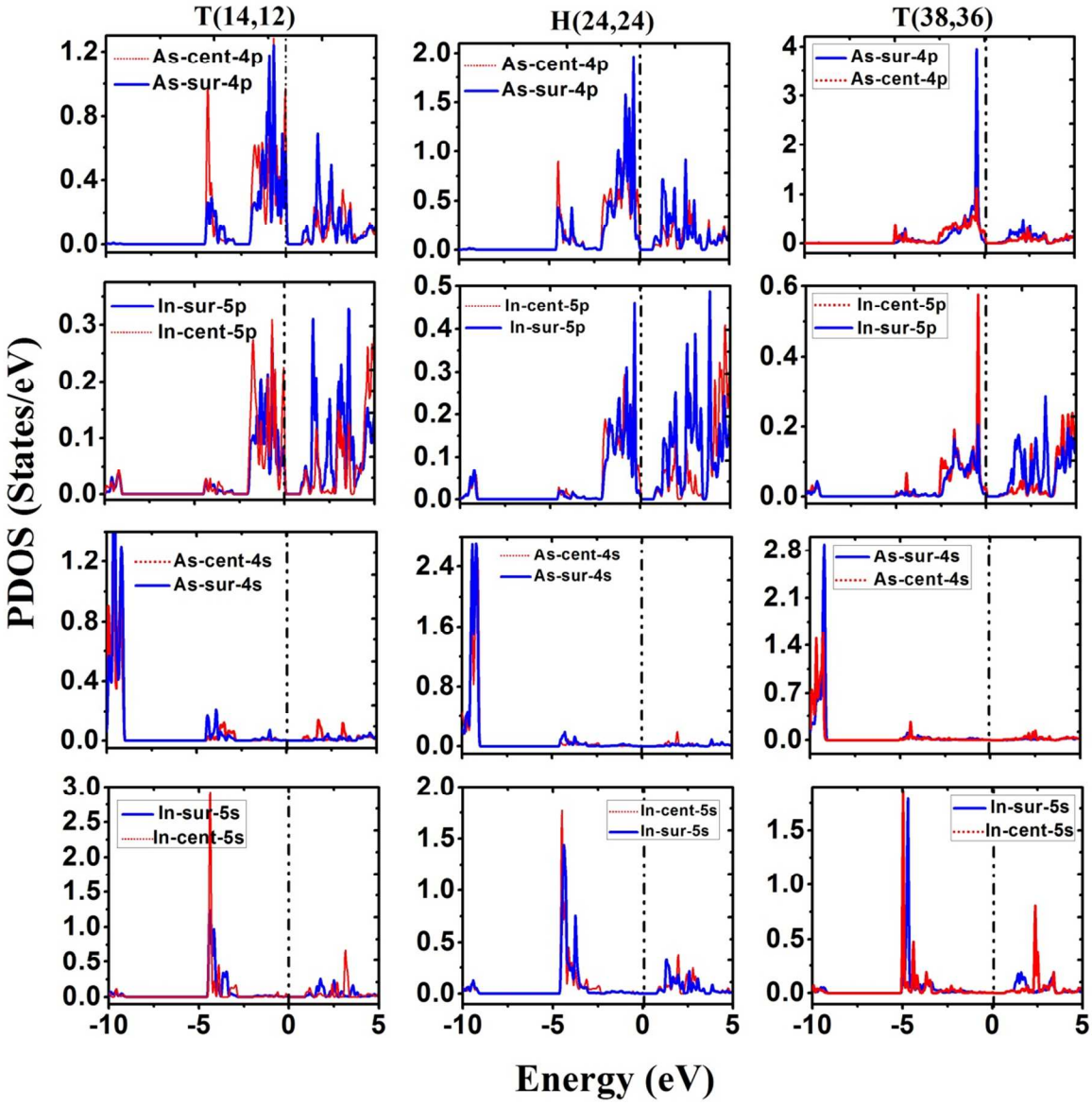

Fig. 10: (Colors online) Partial density of states of nanowires.

IV. CONCLUSIONS

The structural and electronic properties of the bulk and nanowires of InAs in the wurtzite phase are studied by using the theoretical approach of the density functional theory (DFT). We have considered nanowires in the [0001] direction with diameter less than 17.20 Å and then extrapolated our results for larger diameters by using two models. The structural properties calculated by the LDA approach for the bulk sample are in good agreement with the experiments, while the band-gaps for both, bulk and nanowires, are better estimated by the

Engel-Vosko GGA approximation. The results of the NWs conclude that the valence band maximum (VBM) is a nondegenerate level with a high energy dispersion, while the level immediately below in energy (VBM-1) is also nondegenerate but has low energy dispersions. Compared with the bulk InAs, it is observed that the VBM andVBM-1 are nondegenerate for nanowires, such as H(54,54). Except for T(38,36) nanowires, the levels at the top of the valence band have a great dispersion. The observed energetic order inversion at the VBM, from a low energy dispersion level in the NWs, seems to be a general behavior of the III-V NWs. By plotting the total and partial DOS for the s and p orbitals of the center and surface atoms, we conclude that the behavior of the highest occupied (HO) states do not change for all nanowires. In other words, the peak of surface states lies below the valence band maximum and most likely this can be the cause of the less reduced band-gap with respect to the bulk value. The partial density of states show that for VB1 the 4p orbital of As overlaps with the 5p orbital of In, while VB2 is formed by the overlap of 4s orbital of As and 5s orbital of In. Because of the dangling-bonds on the surface, the average energy of the surface states is larger than the center states. An interesting shift in the band-gap from direct to indirect is observed in these NWs with the increase in the diameters of the wires.

ACKNOWLEDGMENTS

We are thankful to Farhad Jalali for his friendly graphical assistance. This work is supported by the Office of Graduate Studies, University of Isfahan (UI), Isfahan, Iran.

REFERENCES

1. U. Krishnamachari, M. Borgstrom, B. Ohlsson, N. Panev, L. Samuelson, and W. Seifert, Appl. Phys. Lett., 2004, **85**, 2077.
2. A. Kazempour, S. J. Hashemifar, H. Akbarzadeh, Phys. Rev. B, 2009, **79,** 195420.
3. E. C. Heeres, E. P. A. M. Bakkers, A. L. Roest, M. Kaiser, T. H. Oosterkamp, and N. de Jonge, NanoLett., 2007, **7,** 536.
4. A. Razavieh, P. K. Mohseni, K. Jung, S. Mehrotra, S. Das, S. Suslov, X. Li, G. Klimeck, D. B. Janes and J. Appenzeller, ACS Nano, 2014, **8,** 6281.
5. S. Upadhyay, R. Frederiksen, N. Lloret, L. De Vico, P. Krogstrup, J. H. Jensen, K. L. Martinezand J. Nygrd, Appl. Phys. Lett., 2014, **104,** 203504.

6. Y. Jing, X. Bao, W.Wei, C. Li, K. Sun, D.P.R. Aplin, Y. Ding, Z. Wang, Y. Bando, and D. Wang,J. Phys. Chem. C, 2014, **118,** 1696.
7. M. P. Persson and H. Q. Xu, Phys. Rev. B, 2006, **73,** 125346.
8. C. L. dos Santos and P. Piquini, Phys. Rev. B, 2010, **81,** 075408.
9. M. D. Moreira, P. Venezuela, and R. H. Miwa, Nanotechnology, 2010, **21,** 285204.
10. J. M. K. Tomioka, J. Motohisa, S. Hara and T. Fukui, Nano Lett., 2008, **8,** 3475.
11. K. S. T. Akiyama, K. Sano, K. Nakamura and T. Ito, Jpn. J. Appl. Phys., 2006, **45,** 2006.
12. P. Hohenberg and W. Kohn, Phys. Rev. B, 1964, **136,** 864.
13. W. Kohn and L. J. Sham, Phys. Rev., 1965, **140,** A1133.
14. P. Blaha, K. Schwarz, G. K. H. Madsen, D. Kvasnicka, and J. Luitz, WIEN2K: An Augmented Plane Waves and Local Orbitals Program for Calculating Crystal Properties, edited by K. Schwarz, Vienna University of Technology, Austria, 2001.
15. E. Sjostedt, L. Nordstrom, and D. J. Singh, Solid State Commun., 2000, **114,** 15.
16. J. P. Perdew, and Y. Wang, Phys. Rev. B, 1992, **45,** 13244.
17. J. P. Perdew, K. Burke, and M. Ernzerhof, Phys. Rev. Lett., 1996, **77,** 3865.
18. P. Dufek, P. Blaha and K. Schwarz, Phys. Rev. B, 1994, **50,** 1994.
19. arXiv:cond-mat/0609616v2 [cond-mat.mtrl-sci] (2006).
20. Z. Zanolli, F. Fuchs, J .Furthm¨uller, U. Von Barth. F. Bechstedt, Phys. ReV. B,**2007,** 75, 245121.
21. H. Shu, X. Chen, H. Zhao, X. Zhou, and W. Lu. J. Phys. Chem. C, 2010, **114,** 17514.
22. S. Q. Wang and H. Q. Ye, J. Phys.: Condens. Matter, 2002, **14,** 9579.
23. J. Bao, D. C. Bell, F. Capasso, N. Erdman, D. Wei, L. Froberg, T. Martensson, and L. Samuelson, Adv. Mater., 2009, **21,** 3654.
24. C. L. dos Santos, P. Piquini, E. N. Lima, and T. M. Schmidt, Appl. Phys. Lett., 2010, **96,** 043111.
25. F. Wang, H. Yu, S. Jeong, J. M. Pietryga, J. A. Hollingsworth, P. C. Gibbons and W. E. Buhro, ACS Nano, 2008, **2,** 1903.
26. S. Faraji, and A. Mokhtari, Phys Lett. A, 2010, **374,** 3348.